Short Communication

Mitigating street flooding with permeable structures:
A modelling case study

Darrien Y. S. Mah[1*], Rosmina A. Bustami[1], F. J. Putuhena[2], and M. Al Dianty[3]

[1] *Faculty of Engineering, Universiti Malaysia Sarawak,*
Kota Samarahan, Sarawak, 94300 Malaysia

[2] *Pembangunan Jaya Center for Urban Studies,*
Universitas Pembangunan Jaya, Tangerang Selatan, 15413 Indonesia

[3] *GeoHydra Consulting Group Pvt Ltd, Tangerang Selatan, 15413 Indonesia*

Abstract

This paper describes the modelling efforts of placing a permeable street adjacent to flash-flood-causing urban drain so that overflowing floodwaters from the drain could be absorbed by water storage structure under the street. Three types of permeable structures were included in the modelling with porosities of 23, 63 and 86 % representing low, medium and high storage volumes, respectively. By using the Storm Water Management Model developed by the US Environmental Protection Agency, the properties of the three types of permeable structures were implemented in models imitating a commercial center and its drainage system, as a case study. The permeable street was modelled as part of the drainage system, in contrast to conventional roads rarely modelled as such. Local rainfall patterns were then used with the models of the case study, in which water flow characteristics of the drainage systems with and without the permeable structures were analyzed. The first type that involved conventional pavers and aggregates had the least water detention time of 2 hours. The second type that consisted of modular precast concrete units held the water for 5 hours; and the third type that was cast-in-place concrete tank system held the water longer for 6 hours. The longer the time floodwater is detained within a permeable structure, the better the mitigating effects of the street flooding. The second and third types of structures were more promising than the first type. However, choosing either second type or third type would be a case-by-case decision, considering various factors of the flash flood.

Keywords: drain, permeable street, spill, stormwater detention, sustainable development, urban runoff

1. Introduction

Commercial areas are usually compact designs with business premises, streets, parking spaces, and other infrastructure supporting the hustle and bustle of the urban life (Purwanto, Ernawati, & Wijaksono, 2017). Such an area, in the perspective of hydrology, is dominated by built-up surfaces that stop rain waters from infiltrating to the natural soil layer (Finaud-Guyot, Garambois, Dellinger, Lawniczak,

& François, 2019). At times, the urban drains over the area are overwhelmed with the amount of rain waters that cause nuisance flooding (Figure 1). Flooded streets are a common scene, in which the congested urban drains are the culprit along with the conventional water-proof tarred streets (Helderop & Grubesic, 2019; Schiermeier, 2018).

Floodwaters tend to accumulate on the streets once the drains are full (He *et al.*, 2018). Failing to infiltrate to the ground due to the tarred street surfaces, the flood causes inconvenience to the local dwellers. Adding a permeable structure to the street could siphon the floodwaters under the street to alleviate the flooding, and to simultaneously ease the burden of the drains in clearing the flow congestion

(Fronczyk, 2017; Törzs *et al.*, 2019). As such, the permeable structures could augment the existing urban drains during rainy days (Mah, Bustami, Putuhena, & Al Dianty, 2020). A general permeable structure presented in Figure 2 consists of a permeable pavement layer on top, followed by a storage layer underneath the pavement.

Current urban flood mitigation measures are focused on efforts to avoid the overflowing of drains, particularly by enlarging the drain size periodically. It is unsustainable to continue to do so as the rainfalls in the equatorial region are expected to increase due to global warming. Instead, by allowing a permeable street beside the drain to absorb the floodwater would be a proactive defense against flash flooding. Furthermore, a street has a larger surface area than a drain, such that could be manipulated for the said purposes. Before the actual structure is built, the system could be evaluated using computer simulations (Pham *et al.*, 2020; Wang, Mao, Wang, Rae, & Shaw, 2018).

In this paper, the effects of permeable street placed beside overflowing drain are explored using stormwater drainage modelling. The types and locations of permeable structures subjected to the street flooding are expected to play key roles in flood mitigation. As such, exploration into the stormwater characteristics with and without the permeable structures, particularly in terms of floodwater profiles along the flooded street and drain in relation to the types and locations of the permeable structures, provides crucial information.

2. Materials and Methods

2.1 Selected permeable structures

Three selected permeable structures are presented in Table 1, describing the two layers in the general permeable structure (Figure 2). The common feature shared by the three structures is the 300 mm storage layer used in the comparisons of the next section.

PS1 is the conventional paver block pavement, in which the top layer was laid with the standard 80 mm thick pavers. Water seeps through the joints between the pavers to drain into the storage layer filled with aggregates. Depending on the size of aggregates, the voids between them provide storage volume to hold water. In the case of PS1, the aggregate used as the base material had a void ratio of 0.29 that produced a porosity of 23% (Park, Sandoval, Lin, & Kim, 2014).

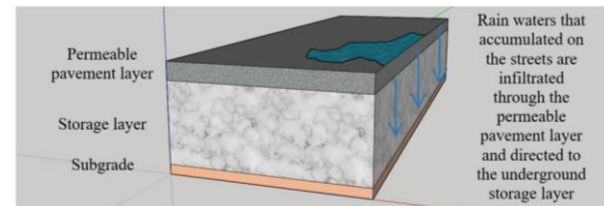Figure 1. Example of flooded street in a commercial area

Figure 2. General permeable structure for urban street

PS2 is a modular-based system, in which pre-cast concrete pieces were set up at the project site. Based on an anonymous product (Mah, Mannan, & Ibrahim, 2018), it has a storage volume of 0.19 m³/m² of pavement area, with a porosity of 63% and solid concrete for the remaining 37%. The storage volume of PS2 was 1.7 fold that of PS1.

PS3 is also made of concrete, but this structure could be built on the spot (cast-in-place) by a construction team. It had the flexibility to have any customized sizes. Following the 300 mm storage layer from the previous two structures, PS3 was estimated to have the largest storage volume of 0.26 m³/m² of pavement area, with a porosity of 86% and solid concrete for a mere 14% (Drake, Young, & McIntosh, 2016).

2.2 Selected commercial area

The three permeable structures described above are set in a commercial area, in the simulations. A study area was pinpointed at a Keranji Square with 42 units of three-story shophouses located in the Kuching city of Sarawak, Malaysia (Figure 3). The total land area measures 10,400 m². Having a study area with measurable site conditions, the setting could be represented realistically in the computer models for investigation (Skrede, Muthanna, & Alfredesen, 2020).

Table 1. Types of selected permeable structures

| Type	Permeable pavement layer	Storage layer	Sourced
Permeable structure 1 (PS1)	Concrete paver Thickness: 80 mm Bedding: 20 mm	Aggregate base course Storage depth: 300 mm Storage volume: 0.069 m³/m² (23%)	Park *et al.*, 2014
Permeable structure 2 (PS2)	Pre-cast concrete plate with inlet Thickness: 75 mm	Pre-cast concrete chamber Storage depth: 300 mm Storage volume: 0.19 m³/m² (63%)	Mah *et al.*, 2018
Permeable structure 3 (PS3)	Cast-in-place concrete slab with inlet Thickness: 100 mm	Cast-in-place concrete wall and base Wall thickness: 25 mm Base thickness: 100 mm Storage depth: 300 mm Storage volume: 0.26 m³/m² (86%)	Drake *et al.*, 2016
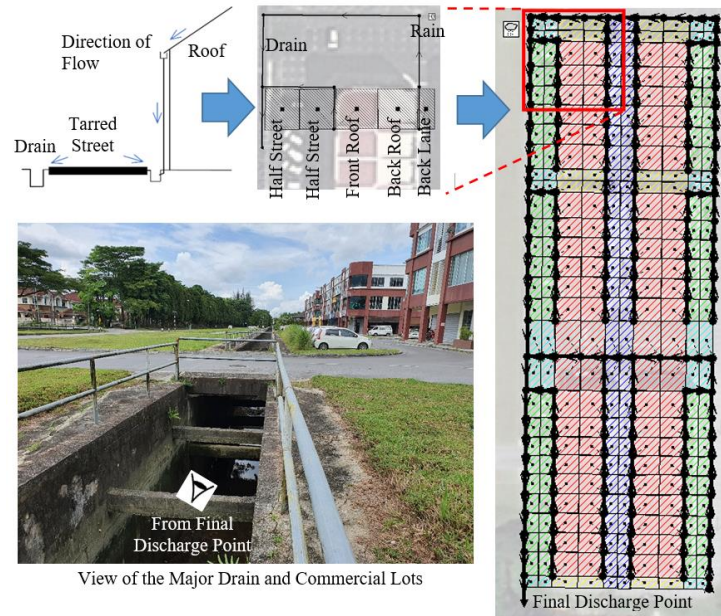
Figure 3.   Modelling approach for conventional drainage system

2.3 Selected modelling software

The selected modelling software is called Storm Water Management Model (SWMM) version 5.0, licensed by the United States Environmental Protection Agency. Generally, SWMM models the rainfall-runoff relationships, in which the rainfall patterns of the study area inserted into model are used to calculate the amount of running water or runoff landed on specific surfaces that are termed catchments. In the urban areas, significant catchments consist of building roofs and streets. The SWMM engine applies nonlinear reservoir representation (Equation 1) (Sadler *et al.*, 2019) to execute the calculation:

$$Q = W \frac{1.49}{n}\left(d - d_p\right)^{5/3} S^{1/2} \tag{1}$$

where,

Q = Water flow from roof or street (m^3/s);
W = Width of roof or street (m);
S = Slope of roof or street (m);
n = Manning roughness value (unitless);
dp = Maximum depression storage (m);
d = Depth of water over the catchment (m).

The runoff eventually is directed into the urban stormwater drainage system. SWMM models the drain network via nodes and links. Nodes represent the features like junctions, bends, and changes of sizes and materials; while links represent the features of the drainage channels. SWMM engine pushes or routs the water along the nodes and links using a kinematic wave approximation (Equation 2) which the SWMM solves numerically (Lee, Hyun, Choi, Yoon, & Geronimo, 2012):

$$q = \frac{\partial A}{\partial t} + \alpha m A^{(m-1)} \frac{\partial A}{\partial x} \tag{2}$$

where,

q = Routed water flow (m^3/s);
A = Cross sectional area of drain (m^2);
x = Distance along the flow path (m);
t = Time (s);
α = Flow geometry due to drain (unitless);
m = Surface roughness of drain (unitless).

The permeable structure could be represented as a node, especially a type of node called Storage Unit in SWMM. This node models the water balance of water flowing in and out of the water storage facility. The computed water flow from Equation 2 is connected to the storage unit as inflow to the storage volume of the permeable structure defined in Equation 3 below:

$$St = \Sigma i(q' - Q_o)\,\Delta t \tag{3}$$

where,

St = Storage volume (m^3);
q' = Inflow (m^3/s);
Q_o = Outflow (m^3/s);
Δt = Duration of storm (s).

Flow leaving the permeable structure is controlled by an orifice outlet. SWMM models the orifice as a node. The outflow, Q_o is the flow from the orifice outlet as defined in Equation 4 below:

$$Q_o = A_o C_o \sqrt{2H_o g} \tag{4}$$

where,

Q_o = Flow from orifice outlet (m^3/s);
A_o = Orifice diameter (m^2);
C_o = Discharge coefficient of orifice (unitless);
H_o = Maximum head to the centre of the orifice (m);
g = Acceleration due to gravity (9.81 m/s^2).

Catchments, nodes and links were digitized in SWMM environment to represent the study area. The authors developed two SWMM models (Figures 3 and 4). The building roofs and streets were divided into small parcels (less than 100 m², and we used 5-minute duration and 10-year ARI (Average Recurrent Interval) design rainfall which was estimated at 278 mm/hr for the two models (Malaysia Department of Irrigation and Drainage, 2012; Singapore Public Utilities Board, 2010).

The conventional drainage model is depicted in Figure 3. Referring to the right side of the figure, polygons with red diagonal lines are roof catchments; polygons with green diagonal lines are front street catchments; and polygons with blue diagonal lines are back lane catchments. Each of these shophouses was measured as 7 m in width and 18 m in length. It can be seen in the figure that the shophouses had two planes of metal roof (polygons with red diagonal lines) of which one plane (70 m²) was inclined to the front, and another one (70 m²) to the back. Similarly, the road catchments were separated into two halves following the road crown that sloped to the sides.

There were two types of concrete drains in the study area, namely 0.5 m x 0.5 m perimeter drains at the front and back of the shops, and 1 m x 1 m drains that surrounded the commercial area. These could be observed as black dots (nodes) and black lines (links) with water flow direction indicated in the figure. Downpipes from the roofs were drained to the 0.5 m x 0.5 m front and back perimeter drains. In this regard, waters from half of the 8 m wide front street (polygons with green diagonal lines) and half of the 4 m wide back lane (polygons with blue diagonal lines) were drained to the perimeter drains as well. These perimeter drains from the six blocks of shophouses and streets were connected to the 1.0 m x 1.0 m major drains (see bottom left of Figure 3) that eventually emptied their water to a stream.

The context of adding permeable structure is depicted in Figure 4. The permeable structure attached to the street was found best modelled as a storage unit with an orifice outlet in SWMM (Mah *et al.*, 2020). This second model basically repeated the first model but with the added storage unit. Referring to the right side of the figure, the storage unit is indicated with a red circle. The characteristics of the selected three permeable structures in Table 1 were input as properties of the storage unit. Therefore, this second model had three sub-models due to the permeable structures. The storage unit excluded the modelling of the permeability of permeable pavement layer and it was assumed that waters could enter the storage layer with ease. The associated flow mechanisms involved urban drains with insufficient carrying capacity to pass floodwaters to the adjacent streets. Floodwaters reaching a designated point of the drain shall be directed to the storage unit that held the floodwaters temporarily and slowly discharged the water back to the downstream drain. Authors added a divider to the drain to cutoff water above 0.30 m³/s at full drain, which was estimated from the conventional drain model. Further descriptions are available in Section 3.1.

2.4 Model verification

The SWMM software has been reported to model permeable roads (Liow, Mah, & Malek, 2019; Liow, Mah, & Mohd Arif Zainol, 2019). Among the parameters in Equation 1, Manning's n-value is a variable, while the other values were measured from the study area. The Manning's n was reported as 0.022 for roof and street surfaces (Mah, Ngu, Taib, & Mannan, 2020). In Equation 2, only the time step is a variable and other values were measured. The routing at a time step of 30 s was applied, starting at the first junction as the upstream boundary and stopping at the final discharge point as the downstream boundary (Sadler *et al.*, 2019). Equation 3 had results from Equations 1 and 2 as inputs, while Equation 4 was related to the characteristics of orifice. Discharge coefficient of the orifice outlet was set at 0.060 (Sadler *et al.*, 2019). As such, model calibration was skipped due to the variables being known from other studies.
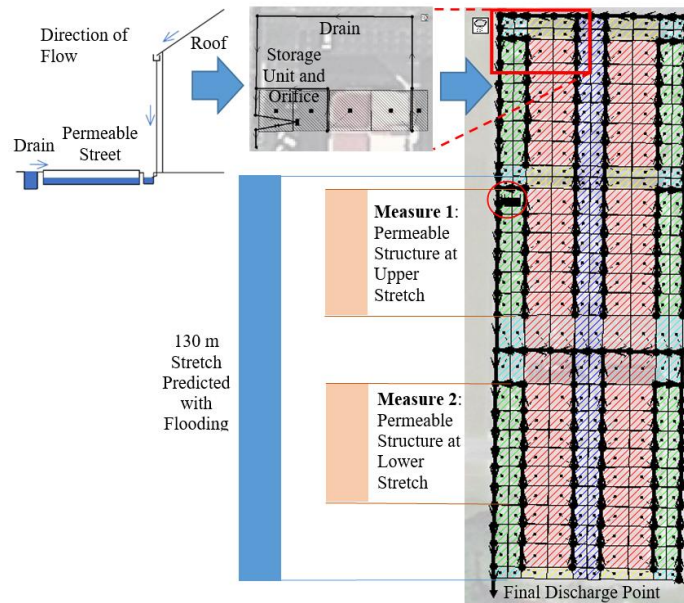

Figure 4. Modelling approach for permeable street beside drain

Model verification was carried out. The verification targeted three major flow processes. Firstly, the modelled runoff from rainfall, termed catchment flow, was verified by using the Rational Method which is traditionally applied for runoff generation from a catchment:

$$Q_{Rational\ Method} = \frac{C.I.A_D}{360} \qquad (5)$$

where,

$Q_{Rational\ Method}$ = Catchment flow (m³/s);
C = Runoff coefficient (unitless);
I = Rainfall intensity (mm/hr); and
A_D = Drainage area (ha).

Secondly, the modelled flow in the urban drain that was termed drain flow and thirdly, the modelled drain flow spilled to the storage unit that was termed storage inflow, were verified using the Manning Equation. The equation is traditionally applied to calculate the flow in the drain and the spill from drain to permeable street:

$$Q_{Manning\ Equation} = \frac{1}{n} A_F R^{2/3} S_F^{1/2} \qquad (6)$$

where,

$Q_{Manning\ equation}$ = Drain flow (m³/s);
n = Manning's roughness coefficient (unitless);
A_F = Flow area of drain (m²);
R = Hydraulic radius of drain (m); and
S_F = Friction slope of drain (m/m).

Hand calculations were done on the three flow processes, in which the theoretical flow values were compared to the SWMM modelled flow rates. These plots are presented in Figure 5. The scatter plots of catchment flows produced a coefficient of determination $R^2 = 0.89$. Looking at the other scatter plots, drain flows produced $R^2 = 0.93$ while storage inflow had $R^2 = 0.94$. These R^2 coefficients exceeded 0.75 indicating good matches.

3. Results and Discussion

3.1 Conventional drainage system

The first SWMM model divided the 10,400 m² commercial area into 280 small catchments, and the waters generated from the catchments were connected to 180 nodes. As such, this model represented the water distribution over the area in detail. Subjected to 5-min, 10-year Average Recurrent Interval (ARI) design rainfall, the model estimated a system-wide peak runoff at 0.8 m³/s. Checking with the Rational Method, the same peak runoff value was calculated.

The 200 m stretch of major drain before the final discharge point (Figure 3) was constructed as a 2 m wide and 3 m deep drain. However, the authors modified the stretch to a smaller 1 m wide and 1 m deep drain in the model to create a flash flooding scenario. The model predicted out-of-drain floodwaters along the 130 m drain before its final discharge point. No flooding was predicted from other minor drains due to the design rainfall.
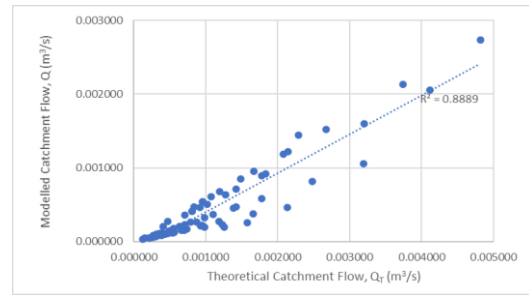
(a)
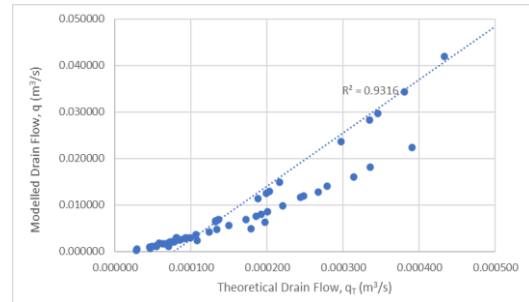
(b)
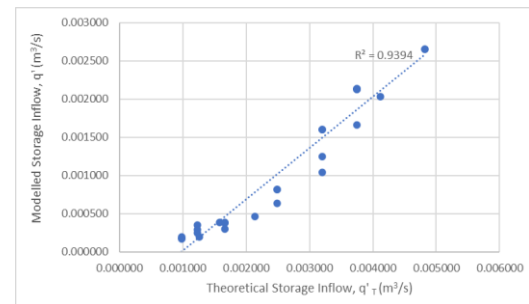
(c)

Figure 5.   Model verification for a) catchment flow, b) drain flow, and c) inflow to storage

The long section views of the selected drain are presented in Figure 6, by time during the event, starting from the onset of the design storm until 30 minutes after the storm had started. The chosen 0 to 30-minute duration managed to capture a complete cycle of water level rise and fall compounded by the drain. The water flowed from right to left as indicated by arrows on the second row of sub-figures. The y-axis shows the 1 m depth of the drain, in which water level reaching the top of the drain indicates flooding. Referring to Figure 6a, the conventional drainage model predicted flooding from 10 to 20 minutes after the onset of the design storm. At 15 minutes, the flooding involved a 130 m stretch from the discharge point; and at 20 minutes, the flooding subsided to involve only an 80 m stretch from the discharge point. As such, the floodwaters would spill on the adjacent street by the drain. The permeable structures should thus be added within the identified 130 m of street from the discharge point.

3.2 Drainage system augmented by permeable street

Two alternative measures of placing the permeable structure are presented in Figure 4, Figure 6b, and Figure 6c. Measure 1 involved the placing of permeable structure at the
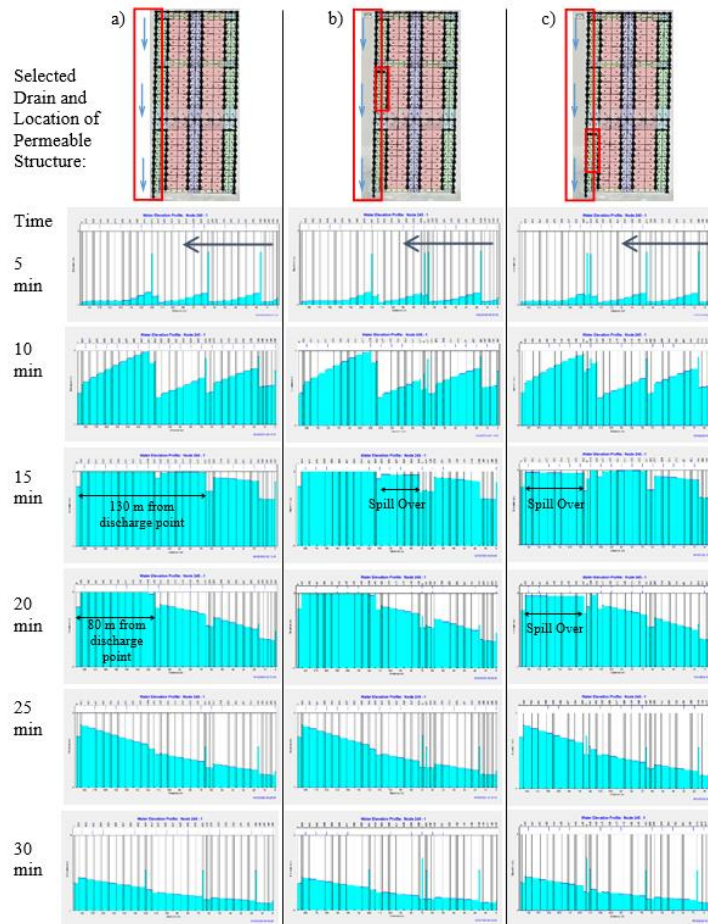
Figure 6.   Predicted flooding along the major drain for a) conventional drainage, b) measure 1, and c) measure 2

upper flooded stretch between 75 and 117 m from the discharge point; while in Measure 2, placement was at the lower flooded stretch between 21 and 63 m from the discharge point. Each permeable structure was maintained at 42 m in length, 8 m in width and 0.3 m in storage depth, and equipped with 0.05 m orifice outlet. Due to the fixed size, regardless of the type of permeable structure inserted in both Measure 1 and Measure 2, the water level plots along the selected drain showed only so small differences (0.002-0.003 m) as to be negligible. Figure 6b is for the three permeable structures according to Measure 1, while Figure 6c is for Measure 2.

In the scenario with Measure 1, when the permeable structure was introduced beside the upper flooded stretch (Figure 6b), floodwater spillover was modelled at the mentioned stretch. Compared with Figure 6a, the upper flooded stretch had flooding in the water level plot at 15 minutes only, and the modelling outcome in Figure 6b is indicated in the plot for the same time frame. A slight drop by 0.04 m of the water level was estimated. This small change in the water level could be observed in the plot. However, in the next plot at 20 minutes, the water level had dropped to non-flooding level. Therefore, the overflow at the stretch was happening for about 5 minutes. Having the permeable structure at the upstream stretch had no impact on the flooding at the downstream stretch. The classic understanding that having an upstream water storage structure could lessen the

flooding at the downstream stretch was not valid in this case. This could be due to the uptake of spillover floodwater being small in quantity (about 0.02 m³/s for the three permeable structures) over a short time span (about 5 minutes) that had little impact on the flood flow (peak value 0.32 m³/s) in the major drain.

Contrary to the former stretch, the lower flooded stretch was found to have flooding in the water level plots from 10 to 20 minutes, for about 10 minutes of out-of-drain flooding in Figure 6a. In the scenario of Measure 2, when a permeable structure was introduced beside the lower flooded stretch (Figure 6c), a drop by 0.04 m of the water level was modelled due to floodwater spillover to the permeable structure. The drop was most visible in the plots at 15 and 20 minutes, in Figure 6c. The next plot at 25 minutes indicated that the water level along the drain had dropped to non-flooding level. Having a downstream water storage structure, in this case, repeated the observation from the previous case, with no sign of lessening the flooding at upstream or downstream of the structure. The reason was again that the uptake of spillover floodwater was in a small quantity (about 0.02 m³/s for the three permeable structures). In this regard, it could also be expected that changes in the hydrographs both in water level and flow were so small that it was hard to discern these variations visually. The hydrograph plots are reasonably skipped in this context.

It was reasoned that if the permeable structure was added along the 130 m flooded stretch instead of being fragmented in the scenarios of Measure 1 and Measure 2, the modelling outcome shall be a combination of the two measures. The permeable structure may cause a slight change in the water level after the floodwater spillover; but overall, the structure had little impact on water level and flow in the major drain.

3.3 Filling of permeable structures

The filling of the permeable structures, on the other hand, varied by the type of the structure. PS1 had the lowest water storage volume, followed by PS2 and PS3 as listed in Table 1. Water levels and their associated water volumes being captured by Measure 1 are presented in Figure 7a. Due to the short flooding time span of the upper flooded stretch, water level and volume readings were generally low. The low-water-storage-volume PS1 was expected to have a smaller hydrograph base and steeper limb than PS2 and PS3. As such, it resulted in a maximum water level of 0.1 m for PS1 that was much higher than the 0.06 m maximum water level reached by both PS2 and PS3. Besides, the average filling percentages over the six-hour simulation were estimated as 16%, 6%, and 4% for PS1, PS2, and PS3, respectively.

Water levels and volumes for Measure 2 are presented in Figure 7b. The water level time series by the type of permeable structure reached the full depth of the structures (0.3 m) due to the longer flooding time span experienced in the lower flooded stretch. Similar patterns as above repeated as regards the upper flooded stretch, in which the low-water-storage volume PS1 had smaller base and steeper limb in its water level hydrograph. PS2 and PS3 that managed to capture more water with wider bases and gentler limbs had a longer time of releasing the captured water. All three permeable structures had reached 100% water volume between 13 and 20 minutes. However, over the six-hour simulation, the average filling percentages were estimated at 13%, 31% and 42% for PS1, PS2 and PS3, respectively.

No plots for Measure 1 are shown, as it had partial filling of the permeable structures that were unimpressive in terms of flood mitigation. In contrast, plots from Measure 2 provided tell-tale signs about the performances of the alternative permeable structures. Referring to Figure 7b

(bottom), PS1 had the smallest triangular-shaped water volume time series and it held the captured water for about two hours. It had the least water detention capability among the three permeable structures. PS2 was able to hold water for about five hours while PS3 was able to do so for about six hours. These two permeable structures had more potential than PS1 to augment the urban drain in dealing with flash flooding. In this case, PS3 with the mentioned 42% average filling percentage appeared as a more efficient system than PS2 with 31%. However, the authors would like to point out that flash flooding events vary significantly, and any mitigation measure should be assessed on a case-by-case basis.

4. Conclusions

SWMM simulation software was used to evaluate the idea of allowing overflowing floodwaters from urban drain to be held in permeable street adjacent to the drain. With a selected commercial area, a flash flooding scenario was created virtually that identified a stretch of flooded street when subjected to 5-min, 10-year ARI design rainfall. Outcomes from the case study indicate that the intended permeable structure should be installed at the downstream section of the flooded stretch to have the investigated flood mitigation be effective, in contrast to the common belief that detention structures should be upstream of the flooded stretch. Three types of permeable structures were investigated. Regardless of the type, the permeable structure had little impact on the flood flow in the drain as only the out-of-drain floodwaters were directed to the structure. Logically, the bigger the water storage volume, the longer the water detention time that is achieved. PS1 with 23% porosity, 13% average filling and two hours water detention time over the six-hour simulation was considered a poorly performing permeable structure. Under the same simulated hydrological hours, PS2 with 63% porosity achieved 31% average filling and five hours of water detention time, while PS3 with 86% porosity achieved 42% average filling and six hours of water detention time. As such, PS2 and PS3 alternatives had more potential than PS1 as permeable structures to receive overflowing floodwaters from urban drains, but such performance generally depends on the site conditions and other factors.
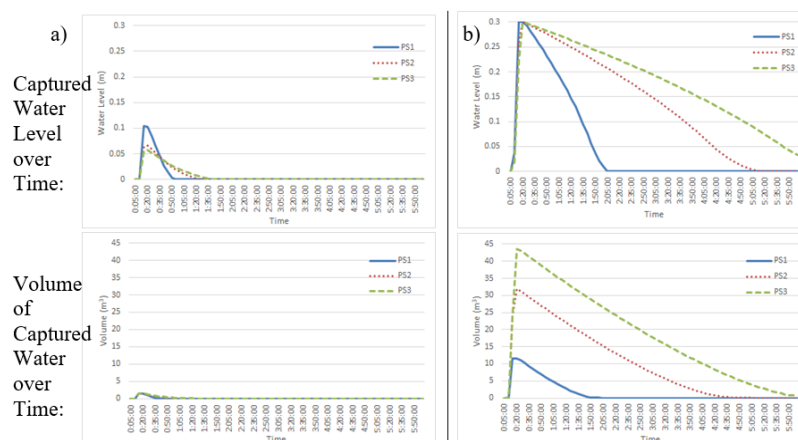

Figure 7. Predicted filling of the permeable structures for a) Measure 1, and b) Measure 2

References

Drake, J., Young, D., & McIntosh, N. (2016). Performance of an underground stormwater detention chamber and comparison with stormwater management ponds. *Water*, *8*(5), article 211.

Finaud-Guyot, P., Garambois, P.-A., Dellinger, G., Lawniczak, F., & François, P. (2019). Experimental characterization of various scale hydraulic signatures in a flooded branched street network. *Urban Water Journal*, *16*(9), 609-624.

Fronczyk, J. (2017). Artificial road runoff water treatment by a pilot-scale horizontal permeable treatment zone. *Ecological Engineering*, *107*, 198-207.

He, B., Huang, X., Ma, M., Chang, Q., Tu, Y., Li, Q., Zhang, K., & Hong, Y. (2018). Analysis of flash flood disaster characteristics in China from 2011-2015. *Natural Hazards*, *90*, 407-420.

Helderop, E., & Grubesic, T. H. (2019). Streets, storm surge, and the frailty of urban transport systems: A grid-based approach for identifying informal street network connections to facilitate mobility. *Transportation Research Part D: Transport and Environment*, *77*, 337-351.

Lee, J.-M., Hyun, K.-H., Choi, J.-S., Yoon, Y.-J., & Geronimo, F. K. F. (2012). Flood reduction analysis on watershed of LID design demonstration district using SWMM5. *Desalination and Water Treatment*, *38*(1-3), 255-261.

Liow, C. V., Mah, D. Y. S., & Malek, M. A. (2019). Modelling of StormPav green pavement system with Storm Water Management Model and SolidWorks Flow Simulation. *International Journal of Recent Technology and Engineering*, *8*(2), 4673-4679.

Liow, C. V., Mah, D. Y. S., & Mohd Arif Zainol, M. R. R. (2019). Modelling of StormPav green pavement system with storm water management model and InfoWorks collective system. *International Journal of Recent Technology and Engineering*, *8*(2), 1449-1452.

Mah, D. Y. S., Bustami, R. A., Putuhena, F. J., & Al Dianty, M. (2020). Testing the concept of mitigating overflowing urban drain with permeable road. *International Journal of Advanced Trends in Computer Science and Engineering*, *9*(5), 7878-7882.

Mah, D. Y. S., Mannan, M. A., & Ibrahim, W. H. W. (2018). Pilot study of stormpav green pavement system. *International Journal of Research in Engineering and Advanced Technology*, *6*(5), 29-35.

Mah, D. Y. S., Ngu, J. O. K., Taib, S. N. L., & Mannan, M. A. (2020). Modelling of compartmentalized household stormwater detention system using SWMM5. *International Journal of Emerging Trends in Engineering Research*, *8*(2), 344-349.

Malaysia Department of Irrigation and Drainage. (2012). *Urban stormwater management manual for Malaysia*. Kuala Lumpur, Malaysia: Ministry of Environment and Water.

Park, D. G., Sandoval, N., Lin, W., & Kim, H. (2014). A case study: Evaluation of water storage capacity in permeable block pavement. *KSCE Journal of Civil Engineering*, *18*(2), 514-520.

Pham, B. T., Avand, M., Janizadeh, S., Phong, T. V., Al-Ansari, N., Ho, L.S., . . . Prakash, I. (2020). GIS based hybrid computational approaches for flash flood susceptibility assessment. *Water*, *12*(3), article 683.

Purwanto, A. N., Ernawati, J., & Wijaksono, A. D. (2017). The factors of land use conversion from settlement area to commercial area at IR. Soekarno/Merr Street, Rungkut Street, and Medokan Ayu Street, Surabaya. *International Journal of Environment and Agriculture Research*, *3*(4), 86-93.

Sadler, J. M., Goodall, J. L., Behl, M., Morsy, M. M., Culver, T. B., & Bowes, B. D. (2019). Leveraging open source software and parallel computing for model predictive control of urban drainage systems using EPA-SWMM5. *Environmental Modeling and Software*, *120*, 104484.

Schiermeier, Q. (2018). Droughts, heatwaves and floods: How to tell when climate change is to blame. *Nature*, *560*(7717), 20+.

Singapore Public Utilities Board. (2010). *Technical guide for on-site stormwater detention tank systems*. Singapore: National Water Agency.

Skrede, T. I., Muthanna, T. M., & Alfredesen, K. (2020). Applicability of urban streets as temporary open floodways. *Hydrology Research*, *51*(4), 621-634.

Törzs, T., Lu, G., Monteiro, A. O., Wang, D., Grabe, J., & Oeser, M. (2019). Hydraulic properties of polyurethane-bound permeable pavement materials considering unsaturated flow. *Construction and Building Materials*, *212*, 422-430.

Wang, R.-Q., Mao, H., Wang, Y., Rae, C., & Shaw, W. (2018). Hyper-resolution monitoring of urban flooding with social media and crowdsourcing data. *Computer and Geosciences*, *111*, 139-147.